



**HAL**  
open science

## Gold(I)-Silver(I)-calix[8]arene complexes, precursors of bimetallic alloyed Au-Ag nanoparticles

Marie Clement, Ibrahim Abdellah, Cyril Martini, Frederic Fossard, Diana Dragoë, Hynd Remita, Vincent Huc, Isabelle Lampre

► **To cite this version:**

Marie Clement, Ibrahim Abdellah, Cyril Martini, Frederic Fossard, Diana Dragoë, et al.. Gold(I)-Silver(I)-calix[8]arene complexes, precursors of bimetallic alloyed Au-Ag nanoparticles. *Nanoscale Advances*, 2020, 10.1039/D0NA00111B . hal-02565496v2

**HAL Id: hal-02565496**

**<https://hal.science/hal-02565496v2>**

Submitted on 23 Nov 2021

**HAL** is a multi-disciplinary open access archive for the deposit and dissemination of scientific research documents, whether they are published or not. The documents may come from teaching and research institutions in France or abroad, or from public or private research centers.

L'archive ouverte pluridisciplinaire **HAL**, est destinée au dépôt et à la diffusion de documents scientifiques de niveau recherche, publiés ou non, émanant des établissements d'enseignement et de recherche français ou étrangers, des laboratoires publics ou privés.

## Gold(I)-Silver(I)-calix[8]arene complexes, precursors of bimetallic alloyed Au-Ag nanoparticles

Received 00th January 20xx,  
Accepted 00th January 20xx

Marie Clément,<sup>a,b</sup> Ibrahim Abdellah<sup>b</sup>, Cyril Martini,<sup>b</sup> Frederic Fossard,<sup>c</sup> Diana Dragoie,<sup>b</sup> Hynd Remita, Vincent Huc<sup>b</sup> and Isabelle Lampre<sup>\*a</sup>

DOI: 10.1039/x0xx00000x

In this paper, we report the first synthesis and characterisations of bimetallic gold(I)-silver(I) calix[8]arene complexes. We show that the radiolytic reduction of these complexes leads to the formation of small bimetallic nanoparticles with an alloyed structure, as evidenced by XPS, HR-TEM and STEM/HAADF-EDX- measurements.

www.rsc.org/

### Introduction

In the last decades, research involving metal nanoparticles (NP) have seeped into many domains: material science, analytical chemistry, biochemistry... Indeed, due to their unique properties, metal NPs find applications in different fields, for instance catalysis, optics, sensing or medicine. However, their properties depend on their size, shape and morphology, parameters which need to be controlled. For that, the use of ligands, capping agents or supports is often required. But, the NP surface and its interactions with the environment and/or the ligands play an important role for applications. Among the ligands, macrocycles such as calixarenes have attracted attention due their conformational behaviour, functionalisation tunability, host-guest properties as well as non-toxicity, biological mimics and surface accessibility. Calixarenes-based NPs have already been the subject of several reviews<sup>1-4</sup>.

Lately, we reported the radiolytic synthesis of mono and bimetallic gold-silver nanoparticles (NPs) stabilised by octa(hydroxyl)-octa(mercaptobutoxy)calix[8]arenes (**C8**, chart 1).<sup>5</sup> For a metal/calixarene ratio of 10, the reduction of metallic salts, AgClO<sub>4</sub> or HAuCl<sub>4</sub>, in the presence of **C8** in ethanolic solution leads to the formation of small spherical NP, homogeneous in size (diameter <5 nm). In the case of the reduction of ethanolic solution containing both Au(III) and Ag(I) salts in the presence of **C8**, alloyed Au-Ag NPs. were obtained with a mean size of 3.5 nm. However, the proportions of gold and silver were not constant from one NP to another and the NP structure appears non-homogeneous with domains containing more gold atoms and others more silver atoms. Such

non-homogeneous structure might come from aggregation of small clusters with different compositions. The variations in the composition might result from different initial complexations between Au(III), Ag(I) and calix[8]arenes. In order to get a better control of the initial complexation between metallic ions and calixarenes, we undertook the synthesis of calix[8]arene-based metallic complexes. First, trimethylphosphine Au(I)-appended calix[8]arene containing eight and sixteen equivalents of gold (**Au(I)-C8** and **2Au(I)-C8**, chart 1) were synthesised and characterised by <sup>1</sup>H and <sup>31</sup>P NMR spectroscopy.<sup>6</sup> We also showed that the radiolytic reduction of these complexes leads to the formation of small Au NPs. This has prompted us to prepare bimetallic complexes with eight equivalents of gold and eight equivalents of silver, and to reduce them to produce bimetallic NPs. Even if several metallo calixarenes have already been reported in the literature,<sup>7-14</sup> few have been used as precursors of NPs or clusters, and to our knowledge none corresponds to bimetallic complex and NP. For instance, Chen et al used Co<sub>16</sub>-calix[4]arene to promote the nucleation and growth of Co NPs under solvothermal conditions.<sup>14</sup> A. Katz and co-workers synthesised gold clusters via NaBH<sub>4</sub> reduction of different Au(I)-calix[4]arene complexes bearing one or two metallic centres.<sup>10-11</sup> They showed the formation of small clusters (< 1.6 nm in diameter) with a small influence of the calixarene conformation and lower rim substituents and they also quantified the accessibility of the gold surface by steady-state fluorescence measurements.

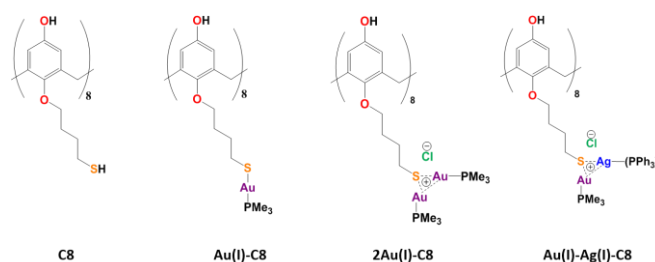


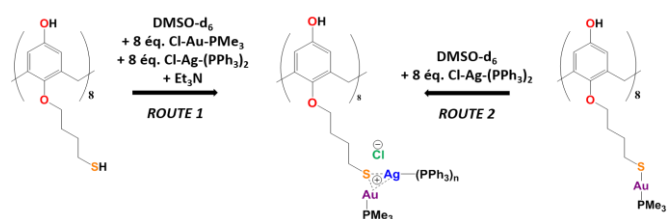
Chart 1 Structures of the calix[8]arenes involved in this study

<sup>a</sup> Université Paris-Saclay, CNRS, Institut de Chimie Physique, UMR 8000, 91405 Orsay, France. E-mail: Isabelle.lampre@u-psud.fr

<sup>b</sup> Université Paris-Saclay, CNRS, Institut de Chimie Moléculaire et des Matériaux d'Orsay, UMR 8182, 91405 Orsay, France.

<sup>c</sup> Université Paris-Saclay ONERA, CNRS, Laboratoire d'Etude des Microstructures, 92322 Châtillon, France

\*Electronic Supplementary Information (ESI) available: [details of any supplementary information available should be included here]. See DOI: 10.1039/x0xx00000x



Scheme 1 Synthetic routes of Au(I)-Ag(I) calix[8]arene complexes

Herein, we report the first synthesis of bimetallic Au(I)-Ag(I)-calix[8]arene complexes with eight equivalents of each metal based on our recent study on Au(I)-calix[8]arene complexes. Then, we investigate the radiolytic reduction of these complexes in ethanolic solution. The formed NPs are characterised by high-resolution transmission electron microscopy (HR-TEM), X-ray photoelectron spectroscopy (XPS) and scanning transmission electron microscopy / energy dispersive X-ray spectroscopy (STEM/EDX). We show that the reduction of Au(I)-Ag(I)-calix[8]arene complexes generates homogeneously-alloyed Au-Ag NPs.

## Results and discussion

### Synthesis of Au(I)-Ag(I)-calix[8]arene complex

The Au(I)-Ag(I)-calix[8]arene complex (**Au(I)-Ag(I)-C8**, chart 1) was synthesised directly in the NMR tube using two routes starting from either **C8** or **Au(I)-C8** (Scheme 1). In the first route **R1**, to a DMSO- $d_6$  solution containing **C8**, were added eight equivalents of Cl-Au-PMe<sub>3</sub> per calixarene molecule and eight equivalents of Cl-Ag-(PPh<sub>3</sub>)<sub>2</sub>. Then, triethylamine (Et<sub>3</sub>N) was introduced to deprotonate the thiol group to facilitate the metal coordination. In the second route **R2**, eight equivalents of Cl-Ag-(PPh<sub>3</sub>)<sub>2</sub> were added to a DMSO- $d_6$  solution of the already synthesized monometallic Au(I)-calixarene complex, **Au(I)-C8**.

Fig. 1 presents the <sup>1</sup>H NMR spectra of Au(I)-Ag(I)-calix[8]arene complexes obtained by the two synthetic routes **Au(I)-Ag(I)-C8\_R1** and **Au(I)-Ag(I)-C8\_R2** (Fig. 1 c and d) as well as those of the initial calixarenes **C8** and **Au(I)-C8** (Fig. 1 a and b). Whatever the synthetic procedures, the spectra of the **Au(I)-Ag(I)-C8** are complex but close as they present broad peaks at similar chemical shifts. The comparison with the initial compounds allow to retrieve the characteristic peaks of the calix[8]arene structure. For the metallic complexes, **Au(I)-C8** and **Au(I)-Ag(I)-C8**, the signal due to thiol group ( $\delta = 2.08$  ppm) is absent, confirming the coordination of the metallic centres to the sulphur atoms. The addition of the metal centres induces a broadening of the peaks indicating a loss in the flexibility of the molecule. The main aromatic resonances observed around 6.3 ppm for **Au(I)-C8** disappear in favour of two broad signals around 5.9 and 6.5 with the addition of Ag(I)-(PPh<sub>3</sub>)<sub>2</sub> revealing a lowering of the symmetry of the formed **Au(I)Ag(I)-C8** complexes, as already noted in the case of the previously synthesized **2Au(I)-C8** complexes.<sup>6</sup> Moreover, in the case of **Au(I)-Ag(I)-C8\_R1**, the spectrum shows more resolved peaks compared to **Au(I)-Ag(I)-C8\_R2** suggesting more rigid

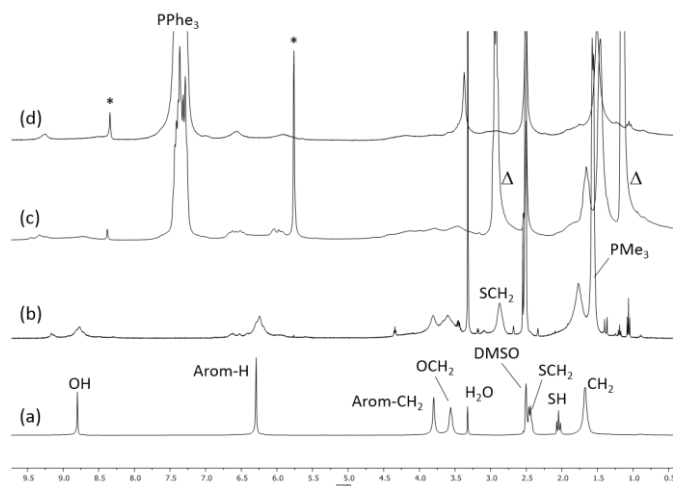


Fig. 1 <sup>1</sup>H NMR spectra of the initial calix[8]arene compounds **C8** (a) and **Au(I)-C8** (b) and those of the gold-silver calix[8]arene complexes **Au(I)-Ag(I)-C8\_R1** (c) and **Au(I)-Ag(I)-C8\_R2** (d) obtained by two different synthetic routes (Scheme 1);  $\Delta$  indicates the peaks corresponding to trimethylamine and \* marks CHCl<sub>3</sub> and CH<sub>2</sub>Cl<sub>2</sub> impurities.

conformers. The presence of Et<sub>3</sub>N in excess in the case of the route **R1** might account for such results. Indeed, the presence of Et<sub>3</sub>N has also an effect on the <sup>31</sup>P NMR spectra of the compounds (Fig. 2). The <sup>31</sup>P spectra of both **Au(I)-Ag(I)-C8\_R1** and **Au(I)-Ag(I)-C8\_R2** differ from those of the metallic precursors, Cl-Au-PMe<sub>3</sub> and Cl-Ag-(PPh<sub>3</sub>)<sub>2</sub>, corroborating the complexation and the absence of free precursors in solution (Fig. 2). The spectra of **Au(I)-Ag(I)-C8\_R1** and **Au(I)-Ag(I)-C8\_R2** also differ slightly from each other, with the main peaks observed at 5 and 7.5 ppm for **Au(I)-Ag(I)-C8\_R1** and **Au(I)-Ag(I)-C8\_R2**, respectively. The possibility of an exchange between a phosphine linked to the metal and triethylamine as a co-ligand (Scheme 2) as well as the formation of triethyl ammonium chlorohydrate could lead to a change in the solvation sphere of the calixarene complexes and account for different <sup>31</sup>P spectra.

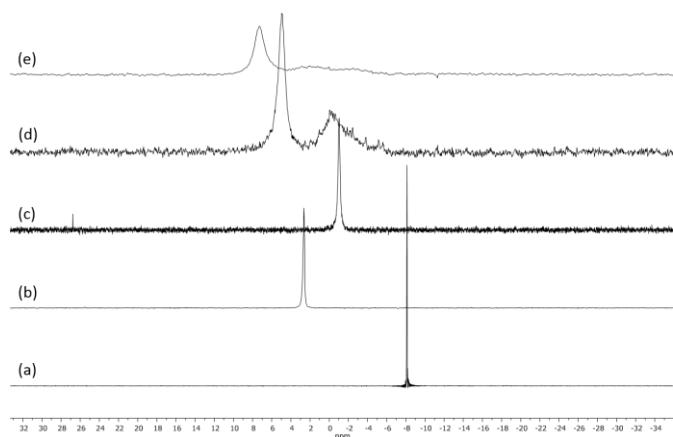
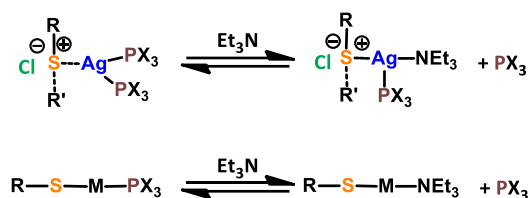


Fig. 2 <sup>31</sup>P NMR spectra of the precursor compounds Cl-Au-PMe<sub>3</sub> (a), Cl-Ag-(PPh<sub>3</sub>)<sub>2</sub> (b) and **Au(I)-C8** (c) and those of the gold-silver calix[8]arene complexes **Au(I)-Ag(I)-C8\_R1** (d) and **Au(I)-Ag(I)-C8\_R2** (e), obtained by two different synthetic routes (Scheme 1).



**Scheme 2** Possible exchanges between phosphine and triethylamine as metal ligand

### Reduction of Au(I)-Ag(I) calix[8]arene complexes

The **Au(I)-Ag(I)-C8\_R1** synthesized *in situ* in DMSO- $d_6$  were diluted in ethanol and then reduced by gamma-irradiation. After centrifugation, the NPs were analysed by TEM. In Fig. 3, small, well-dispersed, spherical NPs are observed with a narrow distribution in size ( $3.5 \pm 0.6$  nm). While the mean size is similar to that previously reported in the case of bimetallic NPs synthesised from metallic salts ( $\text{HAuCl}_4$  and  $\text{AgClO}_4$ ) and stabilised by **C8**,<sup>5</sup> the size distribution is narrower, indicating a better control of the size with the use of a metallic complex.

XPS characterisations allow to get information on the NPs and their surface. The wide-scan spectrum (Fig. 4) shows the presence of the expected elements: carbon, oxygen, sulphur, silver and gold. It is to note that, due to a high contribution of oxygen from the  $\text{SiO}_2$  support, the XPS spectrum of the O1s core-level was not analysed. The XPS spectra of the C1s, S2p, Ag3d and Au4f core-levels are presented in Fig. 5. The C1s signal corresponds to an asymmetric peak at 285.2 eV, and can be related to three contributions as referred in the literature: C-C bonding in the phenyl group (sp<sup>2</sup> C) at 284.8 eV, C-C bonding in aliphatic chain (sp<sup>3</sup> C) at 285.4 eV and C-O/S bonding at 286.3 eV.<sup>15</sup> It is to note that the ratio of the area under the first two peaks is equal to 1.09, close to the ratio of the number of sp<sup>3</sup> (40) and sp<sup>2</sup> (32) carbon atoms in C-C bonds in the **C8** ligand. The S2p signal appears as a broad asymmetric peak with the contributions of S2p<sub>3/2</sub> and S2p<sub>1/2</sub> at 162.5 and 163.3 eV, respectively. This S2p doublet can be attributed to sulphur bound to metal (Au or Ag) as already referred in the literature.<sup>16-18</sup> The spin-orbit doublet of Ag3d corresponds to two well-defined peaks at 368.3 and 374.3 eV for the contributions of Ag3d<sub>5/2</sub> and Ag3d<sub>3/2</sub>, respectively. This signal can be assigned to zero-valent silver.<sup>19,20</sup> However, a small contribution of more-oxidised silver cannot be excluded as the binding energies reported for Ag<sub>2</sub>S ( $E(\text{Ag}3d_{5/2}) = 368.2^{21}$  eV) and Ag<sub>2</sub>O ( $E(\text{Ag}3d_{5/2}) = 368.6$  eV)<sup>19</sup> are very close in energy. The signal of Au4f is also a spin-orbit doublet but here the two observed peaks at 85.3 and 89 eV are asymmetric and not well-separated. The fitting procedure requires the presence of two doublets. The former

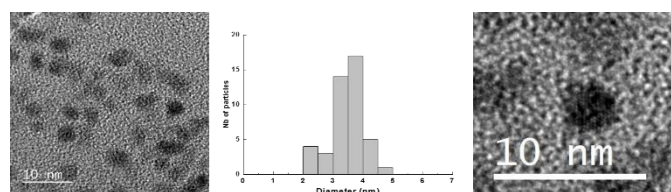


**Fig. 3** HR-TEM images and size distribution of the nanoparticles obtained by radiolytic reduction of **Au(I)-Ag(I)-C8\_R1** complexes

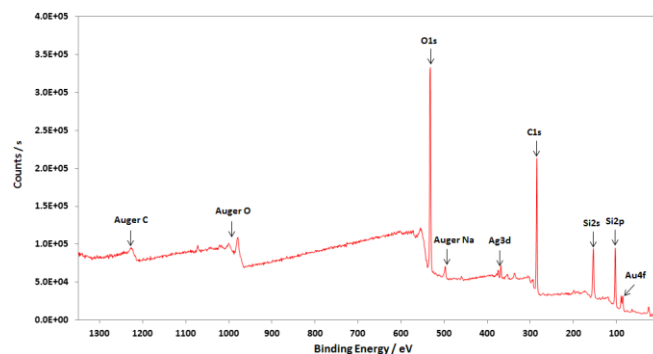


**Fig. 4** Wide-scan XPS spectrum of the nanoparticles obtained by radiolytic reduction of **Au(I)-Ag(I)-C8\_R1** complexes

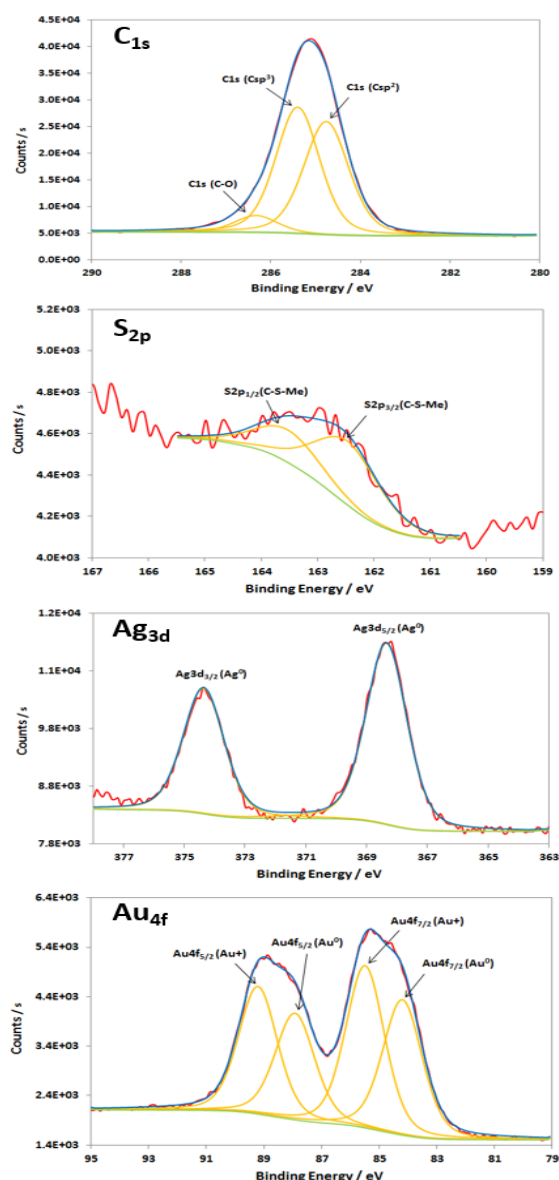


**Fig. 5** XPS spectra of the C1s, S2p, Ag3d and Au 4f core-levels of the nanoparticles produced by radiolytic reduction of **Au(I)-Ag(I)-C8\_R1** complexes

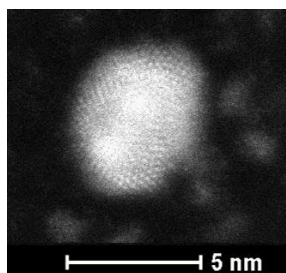


Fig. 6 HAADF-STEM image of nanoparticles produced by reduction of Au(I)-Ag(I)-C8\_R1 complexes

with Au4f<sub>7/2</sub> and Au4f<sub>5/2</sub> contributions at 84.2 and 87.9 eV, respectively, is attributed to metallic gold (Au<sup>0</sup>). The second doublet with components at 85.5 eV (Au4f<sub>7/2</sub>) and 89.2 eV (Au4f<sub>5/2</sub>) corresponds to more oxidised gold and is related to gold atoms bound to sulphur on the NP surface.<sup>20, 22-24</sup> On the whole, the XPS characterisations attest the formation of bimetallic Au-Ag NPs with calix[8]arene ligand grafted on the surface. This result is confirmed by STEM analysis.

Fig. 6 presents the high resolution STEM image in High Angle Annular Dark Field (HAADF) mode. In addition to the expected NPs with sizes around 3.5 nm, the HAADF images reveal the presence of small clusters (< 1 nm in diameter). However, although NPs larger than 4 nm are rare, we select one of them for clarity reasons. Indeed, on the chosen HAADF image, the crystallographic planes of the NP are easily seen (Fig.6). The EDX mapping of two NPs is shown in Fig.7. The superposition of the EDX maps for gold and silver reveals the presence of both metals inside the NPs with a quite homogeneous distribution. The elemental quantification indicates a similar amount of gold (49 ± 3%) and silver (51 ± 3%) atoms, whatever the NP. The EDX map for sulphur also confirm the presence of the calix[8]arene ligands at the surface. Therefore, the reduction of the Au(I)-Ag(I)-C8 complexes leads to the formation of alloyed bimetallic Ag-Au NPs stabilised by calix[8]arenes.

## Conclusions

We have synthesised and characterised by <sup>1</sup>H and <sup>31</sup>P NMR a bimetallic gold(I)-silver(I) calix[8]arene complex. For the first time a fully metallated calix[8]arene with 8 equivalents of Au(I) and 8 equivalents of Ag(I) is reported. The reduction of this bimetallic complex leads to the formation of small spherical bimetallic Au-Ag NPs with an alloyed structure as shown by STEM analysis. It is to note that starting from well-defined bimetallic complexes allows to keep the ratio of the metals for all the produced NPs ([Ag]/[Au] = 1.00 ± 0.12) and to get quite homogeneous structures, in contrast to what was previously observed in the case of the reduction of Au(III) and Ag(I) salts in the presence of calix[8]arenes.<sup>5</sup> The possibility to prepare and reduce calixarene-complexes with others metals allows considering the production of various bimetallic alloyed nanostructures. This can be useful for applications, for instance in catalysis by taking advantage of the synergetic effect of different metals and surface accessibility offered by calixarene ligands.

## Experimental

### Materials

All compounds (silver chloride, AgCl; trimethylamine, Et<sub>3</sub>N; triphenylphosphine, PPh<sub>3</sub>) and solvents (chloroform, CHCl<sub>3</sub>; pentane, C<sub>5</sub>H<sub>10</sub>; ethanol, EtOH; deuterated dimethylsulfoxide, DMSO-d<sub>6</sub>) were purchased with the highest available purity from commercial sources (Sigma-Aldrich and Strem chemicals) and were used without further purification. Argon (Ar, U grade, purity 99 and dinitrogen (N<sub>2</sub>, U grade, purity 99.999%) gases were purchased from Air Liquide.

### Synthetic procedure

The synthesis of *p*-octa(hydroxy)-octa(mercaptobutoxy)-calix[8]arene **C8** and *p*-octa(hydroxy)-octa(mercaptobutoxy)-octa(trimethylphosphine)gold(I)-calix[8]arene (**Au(I)-C8**) have already been described in details elsewhere.<sup>5, 6</sup>

**Bis(triphenylphosphine)silver (I) chloride (Cl-Ag-(PPh<sub>3</sub>)<sub>2</sub>)**. The compound was obtained according to the previously reported procedure.<sup>25</sup> To a suspension of AgCl (1 g, 6.977 mmol, 1 equiv.) in CHCl<sub>3</sub> (150 mL) was added dropwise a solution of triphenylphosphine (7.32 g, 27.91 mmol, 4 equiv.) in CHCl<sub>3</sub> (100 mL). The mixture was kept under stirring at room temperature for 1 h. The mixture was filtered and washed with CHCl<sub>3</sub>. Pentane (250 mL) was added to the filtrate. The mixture was filtered and the solid residue was dried under vacuum. The product was obtained as a white powder in 92 % yield (4.089 g, 6.419 mmol). <sup>1</sup>H NMR (300 MHz, DMSO-d<sub>6</sub>, ppm): δ 7.39 – 7.47 (*m*), 7.37 – 7.26 (*m*). <sup>31</sup>P NMR (300 MHz, DMSO-d<sub>6</sub>, ppm): δ 2.63 (*s*).

***p*-octa(hydroxy)-octa(mercaptobutoxy)-octa(trimethylphosphine)gold(I)-octa(triphenylphosphine)silver(I)-calix[8]arene (Au(I)-Ag(I)-C8)**. **Route R1**. In a NMR tube, to a solution of **C8** (8 mg, 0.005 mmol, 1 equiv.) in DMSO-d<sub>6</sub> (0.3 mL) Cl-Au-PMe<sub>3</sub> (12 mg, 0.04 mmol, 8 equiv.), Cl-Ag-(PPh<sub>3</sub>)<sub>2</sub> (25 mg, 0.04 mmol, 8 equiv.) and then dry Et<sub>3</sub>N (7.7 μL, 0.06 mmol, 12 equiv.) were added under argon. The mixture was sonicated for 2 minutes and heated with a gun for 15 seconds.

**Route R2**: In a NMR tube, to a solution of **Au(I)-C8** (8 mg, 0.002 mmol, 1 equiv.) in DMSO-d<sub>6</sub> (0.3 mL), Cl-Ag-(PPh<sub>3</sub>)<sub>2</sub> (11 mg,

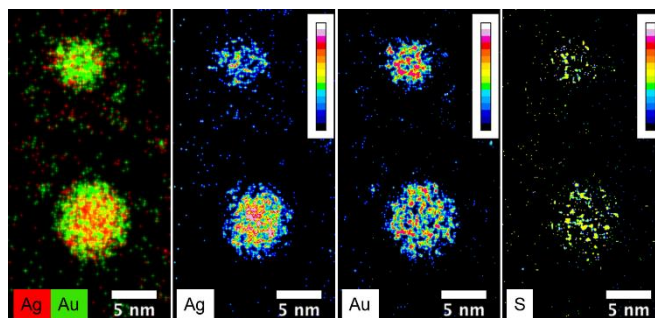


Fig. 7 STEM-EDX maps of silver, gold and sulphur for the nanoparticles produced by reduction of Au(I)-Ag(I)-C8\_R1 complexes, as well as the superposition of silver (red) and gold (green) maps.

0.017 mmol, 8 equiv.) was added under argon. The mixture was sonicated for 2 minutes and heated with a gun for 15 seconds.

#### Radiolytic reduction of Au(I)-Ag(I)-calix[8]arene complexes.

Once synthesised *in situ* and characterised by NMR, the Au(I)-Ag(I)-calix[8]arene complexes in DMSO- $d_6$  were diluted in ethanol to reach a concentration of  $2.5 \times 10^{-5}$  mol L $^{-1}$  (i.e.  $4 \times 10^{-4}$  mol L $^{-1}$  in metallic centres). The ethanolic solution were then deaerated by bubbling with dinitrogen and kept under inert atmosphere during gamma irradiation. The primary effects of the high-energy radiation are the ionisation and excitation of the solvent molecules leading to the subsequent formation of molecule and radical species able to react with the solutes<sup>26, 27</sup>. So, the metallic complexes are reduced till zero-valent metal atoms by the produced solvated electrons and alcohol radicals.<sup>28, 29</sup>

#### Methods and instrumentation

$^1\text{H}$  and  $^{31}\text{P}$  NMR spectra were recorded on Brüker Avance spectrometers at 298 K.

XPS spectra were recorded on a K Alpha (Thermo Fisher) spectrometer, equipped with a monochromatic Aluminum source (Al,  $K_{\alpha} = 1486.6$  eV, beam size: 200  $\mu\text{m}$ ). Wafers were 300 nm thermal SiO $_2$  coated silicon wafers purchased from SiMat. Samples were introduced, without prior surface cleaning. Analysis chamber pressure was  $2 \times 10^{-9}$  mbar. Hemispherical analyzer was used in Constant Analyzer Energy (CAE) mode. Pass energies were 200 eV for the surveys acquisition and 50 eV for the narrow scans. Energies were recorded with a 1 eV path for the survey and 0.1 eV for narrow scans. Charge neutralization is performed by irradiation of the surface with low energy electrons (5 eV maximum).

High-resolution transmission electron microscopy (HR-TEM) images were recorded on a FEI TECNAI F30 microscope operating at an accelerating voltage of 300 kV. The irradiated ethanolic solutions were centrifuged to collect the formed NPs, which were dispersed in propan-2-ol. Droplets of the NPs solution were then deposited onto copper grids coated with an amorphous carbon membrane and dried at room temperature for 20 minutes.

High-angle annular dark field (HAADF) images and energy dispersive spectroscopy (EDX) were performed on a FEI Titan G2 probe-corrected scanning transmission electron microscope (STEM) operating at 200 kV.

The gamma-irradiation were carried out using a panoramic  $^{60}\text{Co}$  source facility. The dose rate, determined by the Fricke method in water solution, was 3.7 kGy h $^{-1}$ . The absorbed dose (576 Gy) was then calculated taking into account the relative electronic density factor of the used solvent (0.8 for ethanol) and adjusted in order to have a total reduction of the metallic complexes.

#### Acknowledgements

The authors thank J.-L. Rodriguez-Lopez and H. Silva at IPiCYT, San Luis Potosi, Mexico, for TEM measurements. HRSTEM-EDX

study was carried out within the MATMECA consortium, supported by the ANR-10-EQPX-37 contract and has benefited from the facilities of the Laboratory MSSMat, UMR 8579 CNRS, CentraleSupélec, Université Paris-Saclay.

#### Notes and references

1. A. Wei, *Chem. Comm.*, 2006, 1581-1591.
2. A. Acharya, K. Samanta and C. P. Rao, *Coord. Chem. Rev.*, 2012, **256**, 2096-2125.
3. V. Montes-Garcia, J. Pérez-Juste, I. Pastoriza-Santos and L. M. Liz-Marzan, *Chem. Eur. J.*, 2014, **20**, 10874-10883.
4. A. R. Kongor, V. A. Mehta, K. M. Modi, M. K. Panchal, S. A. Dey, U. S. Panchal and V. K. Jain, *Top Curr. Chem.*, 2016, **374**, 28.
5. P. Ray, M. Clément, C. Martini, I. Abdellah, P. Beaunier, J. L. Rodriguez-Lopez, V. Huc, H. Remita and I. Lampre, *New. J. Chem.*, 2018, **42**, 14128-14137.
6. M. Clément, I. Abdellah, P. Ray, C. Martini, Y. Coppel, H. Remita, I. Lampre and V. Huc, *Inorg. Chem. Front.*, 2020, DOI: **10.1039/C9QI01475F**.
7. D. M. Homden and C. Redshaw, *Chem. Rev.*, 2008, **108**, 5086-5130.
8. D. Mendoza-Espinosa and T. A. Hanna, *Dalton Trans.*, 2009, 5211-5225.
9. D. Mendoza-Espinosa, A. L. Rheingold and T. A. Hanna, *Dalton Trans.*, 2009, 5226-5238.
10. N. de Silva, J.-M. Ha, A. Solovyov, M. M. Nigra, I. Ogino, S. W. Yeh, K. A. Durkin and A. Katz, *Nature Chem.*, 2010, **2**, 1062-1068.
11. M. M. Nigra, A. J. Yeh, A. Okrut, A. G. DiPasquale, S. W. Yeh, A. Solovyov and A. Katz, *Dalton Trans.*, 2013, **42**, 12762-12771.
12. C. Redshaw, *Dalton Trans.*, 2016, **45**, 9018-9030.
13. B. Ourri, O. Tillement, T. Tu, E. Jeanneau, U. Darbost and I. Bonnamour, *New. J. Chem.*, 2016, **40**, 9477-9485.
14. Z. Chen, J. Liu, A. J. Evans, L. Alberch and A. Wei, *Chem. Mater.*, 2014, **26**, 941-950.
15. J. F. Moulder, W. F. Stickle, P. E. Sobol and K. D. Bomben, *Handbook of X-ray photoelectron spectroscopy*, Perkin-Elmer Corporation (USA), 1992.
16. G. Xue, M. Ma, J. Zhang, Y. Lu and K. Carron, *J. Colloid Interf. Sci.*, 1992, **150**, 1-6.
17. A. J. Leavitt and T. P. Beebe, *Surf. Sci.*, 1994, **314**, 23-33.
18. H. Peisert, T. Chassé, P. Streubel, A. Meisel and R. Szargan, *J. Electron Spectrosc. Relat. Phenom.*, 1994, **68**, 321-328.
19. A. M. Ferraria, A. P. Carapeto and A. M. Botelho de Rogo, *Vacuum*, 2012, **86**, 1988-1991.
20. L. Carlini, C. Fasolato, P. Postorino, I. Fratoddi, I. Venditti, G. Testa and C. Battocchio, *Colloids Surf. A*, 2017, **532**, 183-188.
21. M. Romand, M. Roubin and J. P. Deloume, *J. Electron Spectrosc. Relat. Phenom.*, 1978, **13**, 229-242.
22. A. McNeillie, D. H. Brown, W. E. Smith, M. Gibson and L. Watson, *J. Chem. Soc. Dalton Trans.*, 1980, 767-770.
23. M. P. Casaletto, A. Longo, A. Martorana, A. Prestianni and A. M. Venezia, *Surf. Interface Anal.*, 2006, **38**, 215-218.
24. E. Bedford, V. Humblot, C. Méthivier, C.-M. Pradier, F. Gu, F. Tielens and S. Boujday, *Chem. Eur. J.*, 2015, **21**, 14555-14561.
25. D. V. Sanghani, P. J. Smith, D. W. Allen and B. F. Taylor, *Inorg. Chim. Acta*, 1982, **59**, 203-206.
26. J. C. Russell and G. R. Freeman, *J. Phys. Chem.*, 1967, **71**, 755-762.
27. J. J. Myron and G. R. Freeman, *Can. J. Chem.*, 1965, **43**, 381-394.

28. J. Belloni, M. Mostafavi, H. Remita, J.-L. Marignier and M.-O. Delcourt, *New. J. Chem.*, 1998, **22**, 1239-1255.
29. A. Abedini, A. A. A. Bakar, F. Larki, P. S. Menon, M. S. Islam and S. Shaari, *Nanoscale Res. Lett.*, 2016, **11**, 287.